ISSN 1392–1320 MATERIALS SCIENCE (MEDŽIAGOTYRA). Vol. 25, No. 4. 2019

Comparative Study on the Tribological Properties of AISI52100 Steel Surface Modified by Graphite/MoS_2 Composite Coating and Manganese Phosphate Coating

Libin ZANG [1], Yong CHEN [1]*, Lixin RAN [2], Yang ZHENG [1], Kai LI [1], Dongying JU [3]

[1] *Hebei University of Technology, School of Mechanical Engineering, 300130 Tianjin, China*
[2] *Shell (Shanghai) Technology Limited, 201210 Shanghai, China*
[3] *Saitama Institute of Technology, Fusaiji 1690, Fukaya City, 369-0293 Saitama, Japan*

crossref http://dx.doi.org/10.5755/j01.ms.25.4.19454

Received 10 November 2017; accepted 03 May 2018

Surface modification is an important method to improve the contact fatigue life of transmission parts. The preparation of high performance coating with good tribological properties on the gears and bearings has become the research trends. This paper presents graphite/MoS_2 composite spray and manganese phosphate conversion coating prepared on the AISI52100 steel surface and investigates their anti-fatigue mechanism. The tribological properties of the modified layers were studied using a SRV-IV multifunctional friction and wear tester. The microstructure and interfacial components of the coating and wear surfaces were analyzed by SEM and EDS, respectively. The surface morphology and phase composition of the coating were evaluated through laser 3D microscopy and XRD analyses, respectively. Both modified layers showed good anti-friction and anti-wear properties. The friction coefficients of the surfaces modified by manganese phosphate coating and graphite/MoS_2 decreased by 7 % and 14 %, respectively, and the corresponding extreme pressure properties increased by 11 % and 55 %, respectively. But the mechanism of anti-fatigue wear and the corresponding interfacial phenomena of the surface modification of the graphite/MoS_2 composite spraying layer is different from those of manganese phosphate coating. The hard-ceramic particles with graphite and MoS_2 are sprayed on the substrate to obtain the surface hardening layer, resulting in higher wear resistance. The graphite and MoS_2 modified layer can greatly reduce the friction coefficient and improve the lubrication performance on the surface. Manganese phosphate coating serves as a chemical soft coating and is filled with rough corrugated caused by surface processing, which induces an ideal meshing surface after initial friction phase. The obtained hole-shaped structure and "infiltration" role contribute to the storage of lubricants and thus improves the lubrication performance.
Keywords: surface modification, spraying, electrochemical deposition, tribology.

1. INTRODUCTION

Gear drive is the most important form of mechanical transmission [1]. In this process, gears are subjected to various forces, including bending stress, contact stress, and impact force, which lead to formation of failures, such as tooth flank pitting, spalling, wear, scoring, and tooth bending fatigue [2, 3]. Among these failures, fatigue pitting and scuffing are typical gear damage patterns, which affect transmission and the lifetime and reliability of other driveline systems [4]. Friction and wear occur in mechanical components with contact interfaces. During high-speed rotation movement, high contact stress and meshing speed under repeat forces lead to a certain extent of friction on the gear surface up to the matrix, resulting in gear surface fatigue pitting and scuffing. To solve these limitations, scholars primarily use surface modification for improving the gear anti-fatigue damage capability.

Studies on gear anti-fatigue surface modification have focused on surface coating and shot peening [5 – 13]. Shot peening is a new technology that is categorized into: laser shock peening [8], ultrasonic shot peening [9], fine particle peening [10], and water cavitation peening [11]. Gear surface coating modification commonly utilizes TiN coating [12], MoS_2/Ti membrane [13], and phosphate coating. Lv Y. et al. investigated the effect of shot peening modification and radar surface processing parameters on the fatigue property of 20CrMnTi gear; results showed that the fatigue lifetimes of the LSMSSP gears are grain determined by the retained austenite and surface roughness [5]. Shi et al. studied the influence of manganese phosphate coating on the heat scuffing property of a worm and gear system and found that the manganese phosphate coating can improve the anti-scuffing ability of worm gearing [14]. With the development of transmission systems featuring high strength, high speed, long lifetime, light weight, and downsizing directions, traditional single-surface modification becomes unsuitable and insufficient [4]. Shot peening is an effective method used to improve the anti-bending fatigue property of gear surface but affects the contact fatigue damage on the gear surface. This study aims to investigate the mechanism of the high contact fatigue lifetime of gears and bears with graphite/MoS_2 spray and chemically deposited manganese phosphate coating. Graphite/MoS_2 spray and manganese phosphate coating were prepared on a standard low-carbon alloy steel. The test rig was comprehensively evaluated and compared. The interface microstructure and friction property of the modified layers were analyzed by SEM, XRD, and tribological properties test. The interface

* Corresponding author. Tel.: +86-22-60204241; fax: +86-22-60204241.
E-mail address: *chenyong1585811@163.com* (Y. Chen)

mechanism sunder lying the reduction of anti-fatigue and friction were revealed.

2. MATERIALS AND EXPERIMENTAL

2.1. Substrate

The material components of the test specimens are shown in Table 1, the material is a standard specimen provided by OPTIMOL, and basic information, such as size and surface treatment of the specimens, are illustrated in Table 2. The substrate is a bearing steel (AISI52100, American Standard), which was smelted by vacuum arc D method. The bearing steel is classified as Type A, has a severity level number of 0, 5 (according to Test Methods E45 and Specification A295), and an inclusion sum value of $K1 \leq 10$ (according to DIN EN ISO 683-17). The bearing steel was spheroidized and annealed to obtain globular carbide (62 ± 1 HRC hardness). The surfaces of the disk were lapped and had no lapping raw materials. The topography of the disk was determined by four values: 0.5 μm < Rz < 0.650 μm, 0.035 μm < Ra < 0.050 μm, 0.020 μm < Rpk < 0.035 μm, and 0.050 μm <Rvk < 0.075 μm.

Table 1. Composition of the tested material, wt.%

C	Mn	S	P	Cr	Mo	Ni	Cu	Fe
0.1	0.18	0.02	0.017	1.5	0.08	0.25	0.02	Balance

Table 2. Specimen materials and their treatment conditions

Specimen type	Specimen size	Material	Treatment	Hardness, HRC
disc	Ø 24 × 7.9 mm	GCr15	Quenching (820 ~ 860 °C, oil quenching) Tempering (60 ± 10 °C, 2 ~ 4 h)	61 ~ 63

2.2. Sample preparation

2.2.1. Graphite/MoS_2 modification

A graphite/MoS_2 (PC/MoS_2) layer was prepared as follows. The first type of PC/MoS_2 was prepared mixing the hard- ceramic beads with the solid lubricant in the ejector device. This study selected hard ceramic rolling balls with diameter of 50 μm whose main components of hard ceramic balls are ZrO_2 and SiO_2, where 60 % < ZrO_2 < 70 %, 28 % < SiO_2 < 33 %. MoS_2 and graphite mixture were used as solid lubrication material, and the mass ratio of ceramic balls and solid lubrication is 20:1. The second type of PC/MoS_2 was prepared heating the mixture in the ejector to 300 °C, using inert (N_2, 0 °C) gas under the pressure of 0.4 MPa to push hard particles and solid lubricant onto the surface of the specimen. Hereafter, the surface modification layer sample of PC/MoS_2 was obtained to alter the phase structure of the metal surface at 20 μm in depth [4]. Finally, the ceramic balls were recycled by the recycling device.

2.2.2. Manganese phosphate coating

Electrochemical deposition was employed to prepare manganese phosphate coating (Mn–P coating). Briefly, the steel specimens were cleaned, the substrates were firstly subjected to degreasing treatment at 70 °C ~ 95 °C for 5 min. The degreasing agent was a kind of weak alkaline degreasing agent, whose composition was Na_3PO_4, Na_2CO_3, etc. These samples were separately sonicated in acetone, ethanol and deionized water for 15 min, and dried in N_2 atmosphere. After water cleaning, the surface was modified at 40 to 80 °C and underwent phosphating treatment at 80 ~ 100 °C for 10 to 15 min while controlling the acid ratio between 5.6 and 6.2. The phosphating solution mainly contained of Mn^{2+}、Fe^{2+}, Ni^{2+}, PO_4^{3-}, NO_3^- etc.

2.3. Characteristics

2.3.1. Microstructure characteristics

Morphology and composition were investigated through scanning electron microscopy (SEM, JSM-7100F, Japan) and energy dispersive spectroscopy analyses (EDS). Surface roughness was calculated using a 3D measurement laser microscope (CLSM, OLYMPUS LEXT OLS4000, Japan). The phase composition of the modified layer was investigated by X-ray diffraction (XRD, D8 Focus Bruker AXS, Germany).

2.3.2. Friction coefficient experiment

The tribological properties of PC/MoS_2 and Mn–P coatings were tested on an SRV multifunctional friction test machine (SRV-IV, OPTIMOL, Germany). The equipment and test principle are shown in Fig. 1 The SRV friction test equipment can simulate movement, displacement, and direction of friction contact, including spot contact, linear contact, and face contact; the movement pattern can simulate reciprocal movement and rotation movement and can be applied in lubrication, material, and coating friction analysis. This work used spot contact and the reciprocal movement pattern to measure the sliding friction coefficient of the coatings.

Multi-pass reciprocating sliding tests were carried out in a translator oscillation tribometer (Fig. 2 b), which simulates well the reciprocating movement. The experiment standards according to ASTM standards D7421 and experiment parameters are shown in Table 3. Each test was performed under the same conditions for three times for statistical evaluation. New surface was selected for each test. The property parameters of lubrication oil are shown in Table 4. Before the experiment, to make the surface clean and avoid surface impurities affecting the accuracy of measurement of friction coefficients, all the samples were subjected to ultrasonic cleaning for 15 min with n-heptane before each test and therefore, the tests were done under lubricating of adopts disposable titration 0.3mL of lubrication oil.

Table 3. The friction and wear test parameters

Parameters	Value
Temperature, °C	80
Frequency, Hz	50
Stroke sliding speed average value current, m/s	0.1
Load, N	50/200
Stroke, mm	1
Time, s	6000

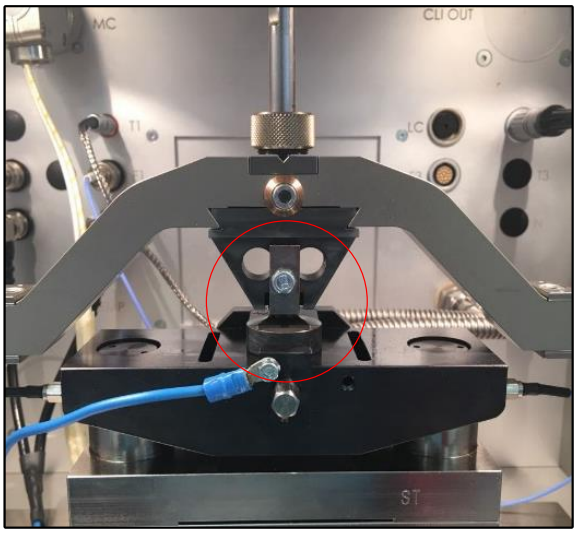

a

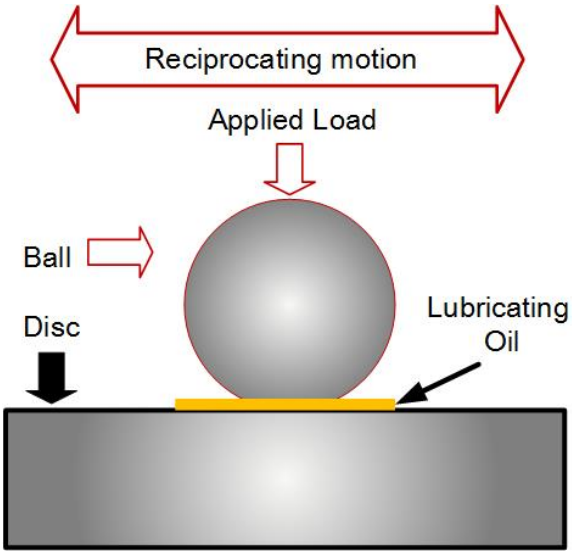

Fig. 1. SRV measurement equipment and measurement principle: a – SRV measurement equipment; b – measurement principle diagram

Table 4. Combination of the oil specifications of an experiment

Factor	DCTF
Density, g·cm^{-3} @15 °C	0.867
Dynamic viscosity, cSt @100 °C	7.55
Mean dynamic friction coefficient	0.128
Lubricating oil volume	0.3 mL

In tribology, the coefficient of friction (f), n is the dimensionless ratio of the friction force (F_f) between two bodies to the normal force (F_n) pressing these bodies together.

$$f = \frac{F_f}{F_n}. \quad (1)$$

2.3.3. Extreme pressure (EP)

The SRV test equipment was used to measure two kinds of surface modification EP properties to evaluate the effect of surface modification methods on the EP property of lubrication oil. In the test procedure according to ASTM D4172, a dynamic test program with the following test parameters was generated. In this dynamic test program, the maximum load range should be set to a maximum of 2000 N with a frequency of 50 Hz for a stroke length of 50 mm. The test temperature of 80 °C and a load of 50 N was applied for 30 s, followed by a load increment of 100 N for 15 min. A load increment of 100 N was then applied every 2 min.

Load carrying capacity can be reported as geometric contact pressure P_{geom} at test end according to the following equation:

$$P_{geom} = \frac{F_N}{\pi W_K^2}, \quad (2)$$

where F_N is normal force (test load); P_{geom} is geometric contact pressure, and W_k is the wear scar diameter.

2.3.4. Observation of morphology after friction

After the friction test, the test parts were ultrasonically cleaned. The surface morphology and element composition of the friction test parts were studied through SEM and EDS.

3. RESULTS AND DISCUSSION

In the present study, Fig. 2 a and b show the results of applying hard micro particles, graphite, and MoS_2 solid lubrication mixture to the coating on the bearing outer ring; this method reduced the pressure marks in the transmission needle bearing and the surface friction [4].

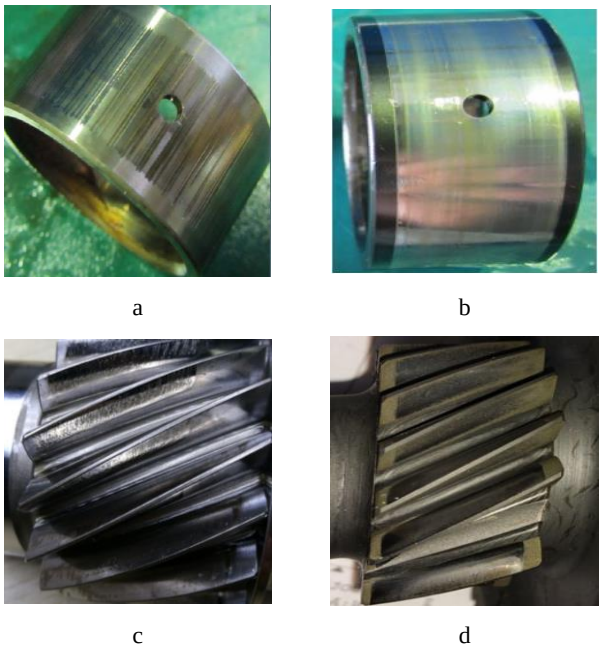

a b c d

Fig. 2. Examples of spray and manganese phosphate coating modification: a – nedle-bearing outer ring prior to treatment macroscopic morphology; b – graphite/MoS_2 after treatment macroscopic morphology; c – gear surface before treatment through testing for 1.2×10^6 cycles; d – manganese phosphate after treatment through 1.2×10^7 cycles

Fig. 2 c and d show the prepared manganese phosphate coating after carburizing and quenching heat treatment. The fatigue experiment results indicated that gear contact fatigue lifetime was enhanced by two to three times after

treatment of the manganese phosphate coating [15, 16]. However, the principles of the two surface treatments and interface analysis remain unclear.

3.1. Surface microstructure

3.1.1. Macroscopic morphology

The matrix samples were treated by two surface modification methods using PC/MoS_2 and Mn–P coating to obtain the surface modification layer. Fig. 3 shows the macroscopic morphologies of manganese phosphate coatings. Evidently, the PC/MoS_2 and Mn–P coatings completely mask the metallic luster of the matrix, and the surface of the manganese phosphate coating is more uniform and denser than that of the PC/MoS_2 surface.

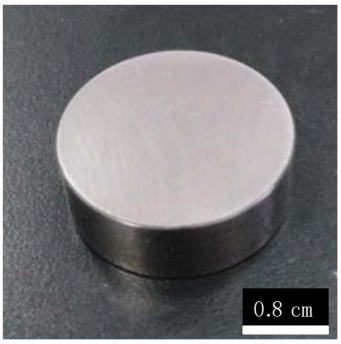

a

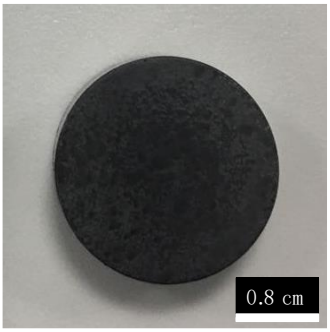

b

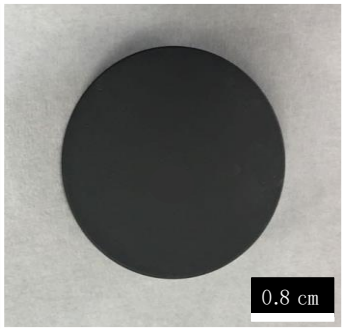

c

Fig. 3. Specimens before and after treatment; a – untreated; b – modified with PC/MoS_2; c – modified with P – Mn coating

3.1.2. Structural examinations

The phase structure on the surface of the coating specimen was analyzed with X-ray diffraction (XRD). Fig. 4 a shows that the main phase of the film obtained after manganese phosphate conversion treatment is manganese phosphate $Mn_3(PO_4)_2 \cdot 3H_2O$. Small amounts of $Mn_2P_4O_{12} \cdot 10H_2O$ and (Fe, Mn)$_2$(PO_4)(OH), and iron oxide were formed on the contact surface between the film and the substrate. The reaction principle of manganese phosphate coating is as follows:

$Mn(H_2PO_4)_2 \leftrightharpoons MnHPO_4 + H_3PO_4$

$Fe(H_2PO_4)_2 \leftrightharpoons FeHPO_4 + H_3PO_4$

$3(Mn, Fe)(H_2PO_4)_2 \leftrightharpoons (Mn, Fe)_3(PO_4)_2 + 4H_3PO_4$

As shown in Fig. 4 b, the PC/MoS_2-modified surface mainly consists of solid lubricants, such as MoS_2 and graphite. The XRD patterns show the successful preparation of two modified layers on the substrate surface.

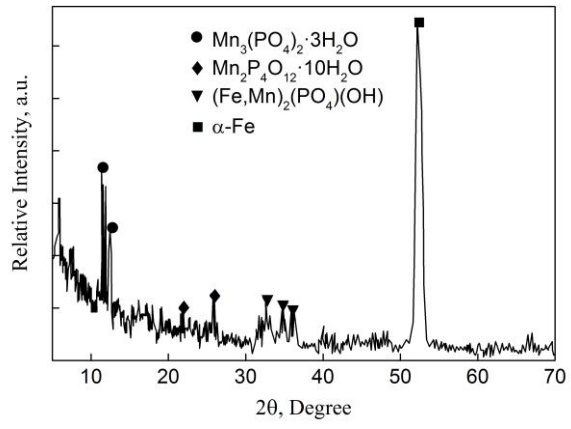

a

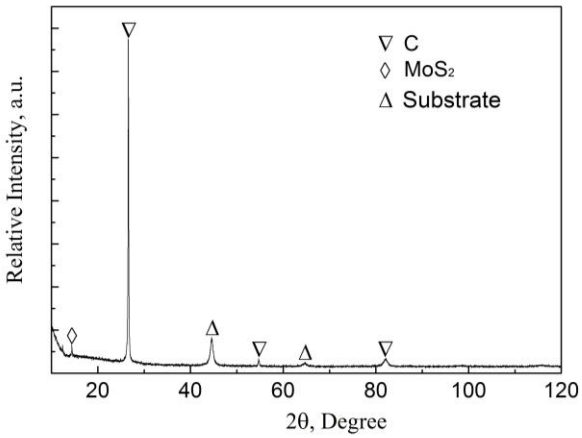

b

Fig. 4. Surface XRD pattern of Mn–P coating and PC/MoS_2: a – phase structure of the Mn – P coating; b – phase structure of PC/MoS_2

3.1.3. Surface morphology

Fig. 5 shows the SEM image (JSM-7100F) indicating the surface morphologies of the surface modified by PC/MoS_2 and Mn-P coatings. The PC/MoS_2-modified layer form sadense solid lubricant and binder, and the coating surface is smooth (Fig. 5 a). The formation of manganese phosphate conversion coating is a chemical conversion process between the steel surface and phosphate solution, and the coating is formed after the reaction between the solution and the substrate [4]. The coating is irregularly arranged with a small amount of voids on the surface. The size of the phosphating grain can be regulated by controlling the reaction process. The grain size of the phosphating film prepared in this experiment is 5 – 7 μm. Based on the equation $Fe+2H^+ \leftrightharpoons Fe^{2+}+H_2$, iron is oxidized by hydrogen ions in acidic solutions, and the neutralization reaction leads to the deposition of small amounts of soluble phosphate. During the reaction, a mixed phosphate is formed due to the substitution of Fe^{2+} with Mn^{2+}.The deposited oxide layer is discontinuous, as verified by the surface micromorphology of the coating.

3.1.4. Surface roughness

The tribological properties of the contact surfaces are directly affected by the surface morphology.

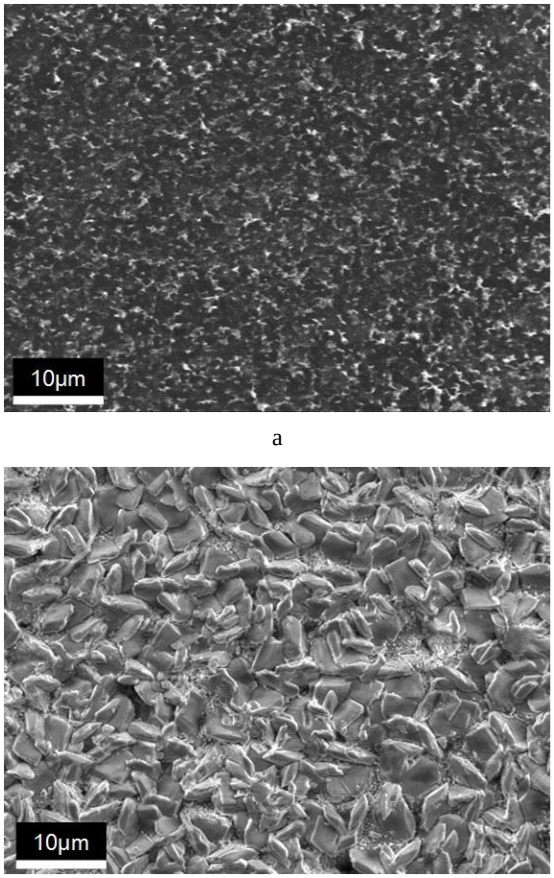

a

b

Fig. 5. Surface topography: a – PC/MoS_2, b – Mn – P coating

Roughness is the most commonly used surface topography parameter that describes the geometrical characteristics of a surface [18]. The effect of the initial friction surface topography on the characteristics of wear performance occurs in two aspects: surface morphology affects the working performance of friction pairs in steady wear stage after running and wear rate affects the working life of friction pairs during the running-in process. Surface roughness significantly influences the lubrication conditions of gears and other contact pairs. The rough surface can reduce the lubricant film thickness between the gears and deteriorate the lubrication conditions. The surface topography of PC/MoS_2 and Mn – P coatings were analyzed using a laser microscope (Fig. 6). The surface roughness of the coatings was then measured three times, and the average value was determined. The line roughness and surface roughness of the PC/MoS_2 surface are Ra = 0.101 μm and Sa = 0.329 μm, respectively, whereas those of the Mn – P coating are Ra = 0.515 μm and Sa = 0.501 μm, respectively. Compared with that of the substrate, the surface roughness after surface modification is slightly improved due to the formation of iron oxides (XRD results). However, the two surface-modified coatings belong to the soft layer, which can reduce the surface roughness after the initial run-in. This finding can be proven by the following friction test.

3.2. Microstructure of section

Fig. 7 shows the surface topography and energy spectra of the PC/MoS_2 surface-modified specimen. The lubricant layer thickness is 8 – 12 μm, and the coating is loosely organized from the cross section (Fig. 7 a). Fig. 7 b, c, and d show the EDS maps of the following elements on the surface: 1 % Mo and 11 % C. Mo, S, and C are present on the interface between the coating and the substrate.

Fig. 8 shows the cross-section topography and distribution of element of the Mn – P coating. As shown in Fig. 8 a, the thickness of the lubricant layer is 5 ~ 7 μm. Based on analysis of the cross section, the coating is compact in structure and bonds well to the substrate. The element matrices of Mn and P diffuse at the interface of the coating and matrix, and the contents of P and Mn are 11 % and 6 %, respectively (Fig. 8 b, c, and d).

3.3. Tribological properties

3.3.1. Friction coefficient

Friction caused by the sliding movement of two gear surfaces leads to fatigue pitting friction and adhesion friction. The sliding friction coefficient is the key tribological property of the surface modification layer [17]. Sliding friction coefficient can be measured to evaluate the tribological performance of the two kinds of surface layers. According to the friction coefficient–time curve, the status and mechanism of the modified surface during friction were further analyzed.

Fig. 9 shows the sliding friction coefficient test curves of the two surface-modified layers, as measured by the SRV friction tester. During the period with a load of 50 N, the specimen friction coefficient decreased after treatment with PC/MoS_2 and Mn – P coating, and the average sliding friction coefficient of the untreated substrate is between 0.150 and 0.155 (Fig. 9). The friction coefficient decreased to 0.05 to 0.1 after the two surface modification processes, and the friction coefficients of PC/MoS_2 and Mn–P coating are basically the same. In the 200 N load grinding stage, the friction coefficient curve decreased, and the friction coefficient of the Mn – P coating decreased by 0.07 – 0.09, or about 7 %, compared with that of the untreated sample. PC/MoS_2 exhibited improved friction reduction performance, and the friction coefficient decreased by approximately 0.2, showing 14 % reduction.

3.3.2. Extreme pressure characteristics

Good extreme pressure property affects gear lifetime. Extreme pressure determines the loading capability of transmission components and lubrication conditions under large alternating loading forces [19]. Extreme pressure property test is used to investigate gear lubrication oil loading and anti-friction capability.

Fig. 10 shows the extreme pressure characteristic curve of the untreated substrate, PC/MoS_2, and Mn – P coating. The extreme pressure load of the untreated specimen is 900 N, and the friction curve is relatively smooth (Fig. 11 a). The extreme pressure load of the Mn – P coating is1000N, the friction curve jumps with a load of 600 N (Fig. 10 b). The phosphate coating possibly formed flakes, with the low friction coefficient and good self-lubricating properties make the two coatings have better extreme pressure characteristics.

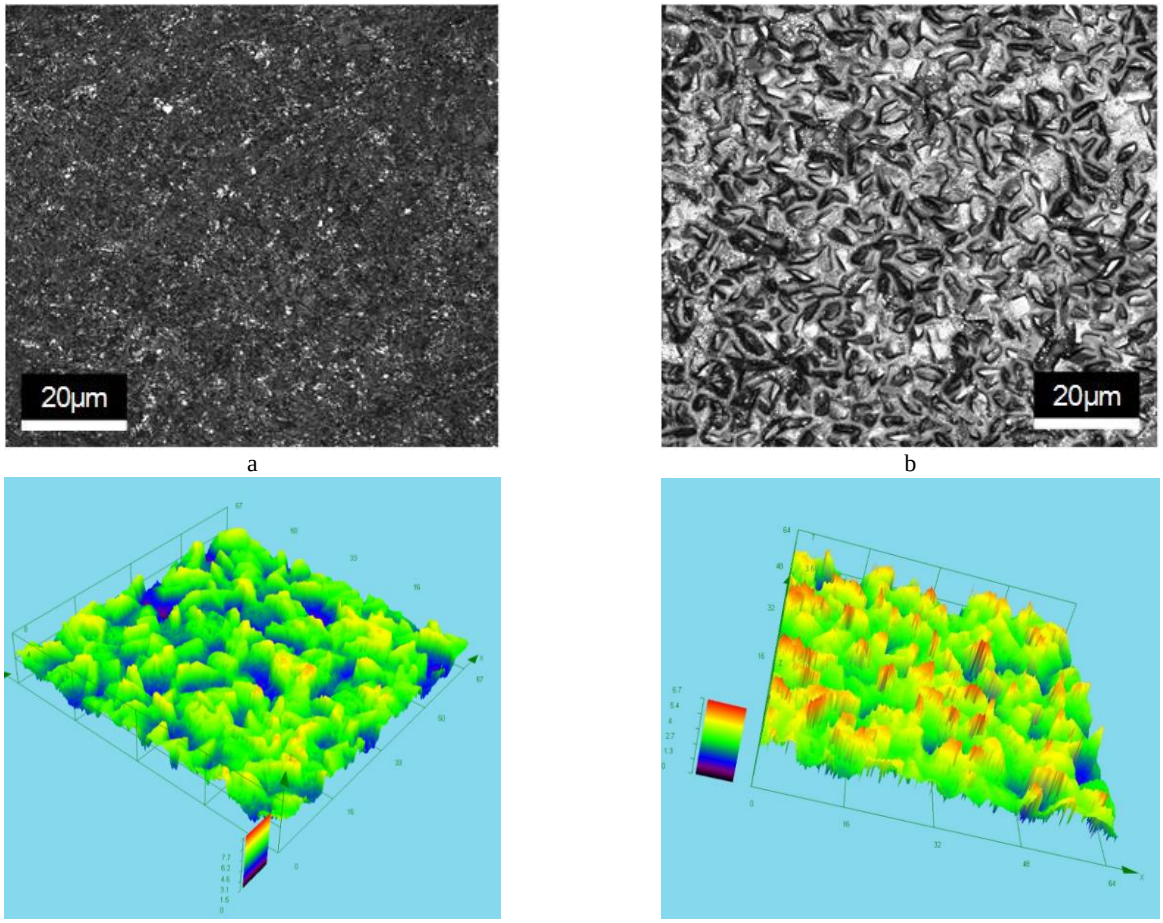

Fig. 6. Three-dimensional topography observation and roughness measurement: a – CLSM picture of PC/MoS_2; b – CLSM picture of the Mn – P coating; c – CLSM three-dimensional topography of PC/MoS_2; d – CLSM topography of the Mn – P coating

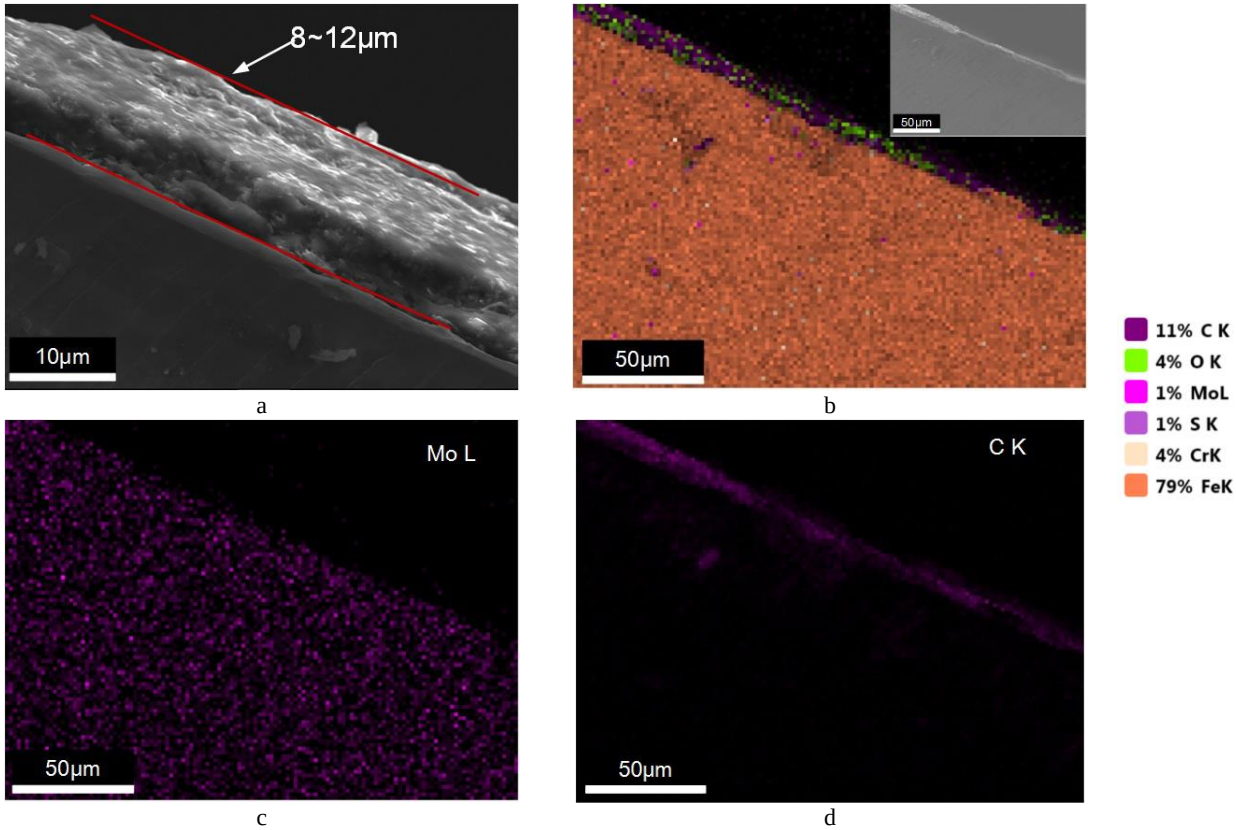

Fig. 7. Cross-section morphology and EDS of PC/MoS_2: a – cross-sectional morphology; b – elemental mapping distribution; c – mapping distribution of Mo element; d – mapping distribution of C element

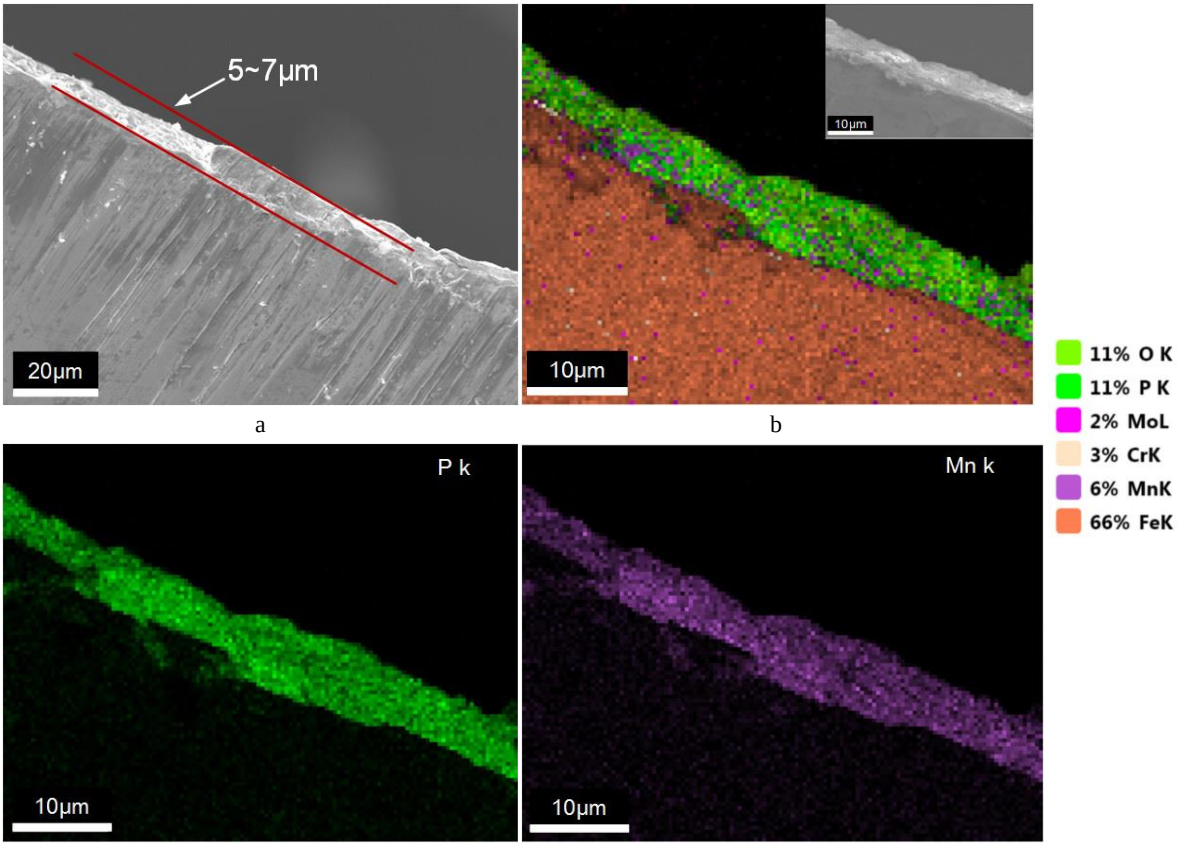

Fig. 8. Cross-section morphology and EDS of Mn-P coating: a – cross-sectional morphology; b – elemental mapping distribution; c – mapping distribution of Mo element; d – mapping distribution of C element

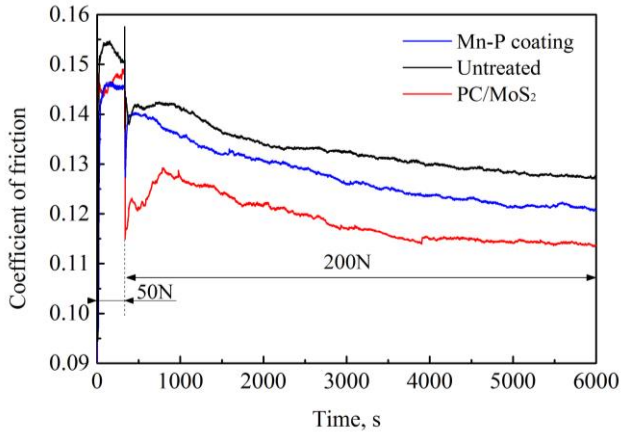

Fig. 9. Friction coefficients of untreated specimens, PC/MoS_2, and Mn – P coating

Fig. 10 c shows that PC/MoS_2 bears a high extreme pressure load of 1400 N.Hence, PC/MoS_2 improves the extreme pressure performance of lubricating oils, and the modified surface exhibits good abrasion resistance.

3.4. Observation of morphology after friction

3.4.1. SEM

Fig. 11 shows the SEM image indicating the surface topography of PC/MoS_2 and Mn-P coating specimens after the friction test. After wear test, the PC/MoS_2 surface lubrication bonding coating is damaged and some of abrasive marks. There's a partial spalling of the coating. (Fig. 11 a). However, the base material of the specimen is protected by the lubrication layer and there is no obvious wear mark. It is assumed that the adhesive wear does not happen on the substrate surface. But the lubricants oil color came black, it is inferred that graphite and MoS_2 solid coatings dissolved into lubricating oils. Moreover, the original trace of friction pairs is clearly visible on the surface, showing markedly improved abrasion resistance of the matrix.

Given that the manganese phosphate modified coating is classified as a chemical combination, the coating shows good bonding property, the surface does not show the peeling phenomenon, and abrasion occurs in the coating. As can be seen from Fig. 11 b, the sliding at a contact load of 200 N after 6000 s produced a smooth wear track with the phosphate coating still present on the substrate.

3.4.2. EDS analysis

Fig. 12 shows the results of the EDS element analysis of the wear surface after wear testing on the two kinds of surface-modified specimens. Fig. 12 a and c show that the S and Mo contents in the PC/MoS_2 wear surface account for 2 %, and the surface of the coating remains to be lubricated by the self-lubricating material. Fig. 12 b and d show the wear marks of Mn–P, and the coating wear surfaces possess high amounts of Mn and P.

3.5. Friction mechanism analysis

Fig. 12 a and c show the element content of a point (EDS) on the PC/MoS_2 coating.

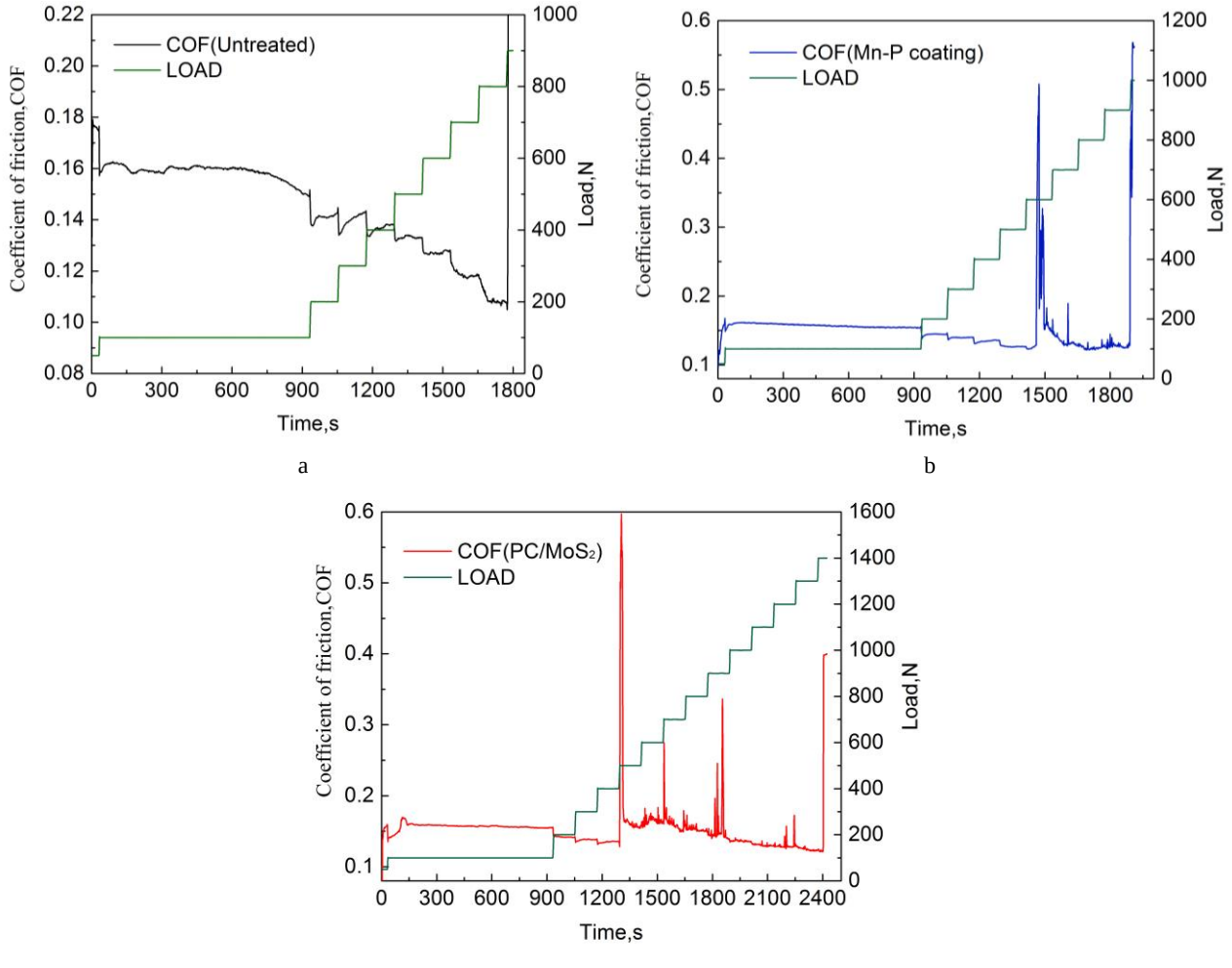

Fig. 10. Extreme pressure characteristics of untreated specimens, Mn – P coating and PC/MoS_2: a – untreated specimens; b – Mn – P coating; c – PC/MoS_2

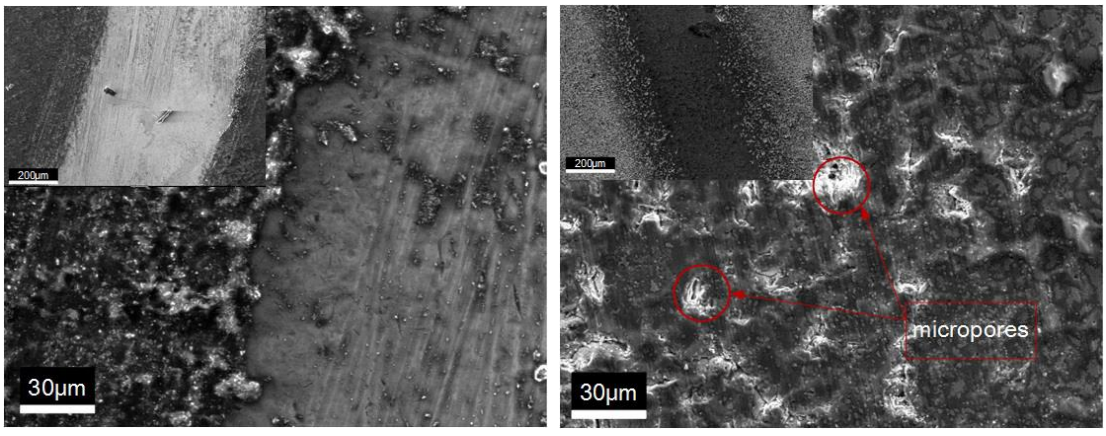

Fig. 11. SEM morphology of PC/MoS_2 and Mn – P coatingafter the friction test: a – PC/MoS_2; b – Mn – P coating

The wear surface contains high amounts of Mo, S, and C. Mo at the interface between the coating and substrate diffuses into the matrix, and a large amount of Mo, S, C, and other elements are enriched at the parent material near the interface. This elemental distribution not only strengthens the matrix but also play the role of antifriction solid lubricant and extreme pressure additive. As seen from the wear morphology, the furrow effect and adhesion wear on the surface become abrasive wear owing to MoS_2, graphite particles fall off, and the transfer of film lubrication occurs. The possible antifriction and antiwear mechanisms are as follows: the solid lubricant, such as MoS_2 and graphite, enters into the friction pair surface, remains in the rough trough or grinding mark of the friction pair surface, and increases the actual contact area of the friction pair surface; the abrasion-generated grinding marks are filled at any time by the MoS_2 solid lubricant.

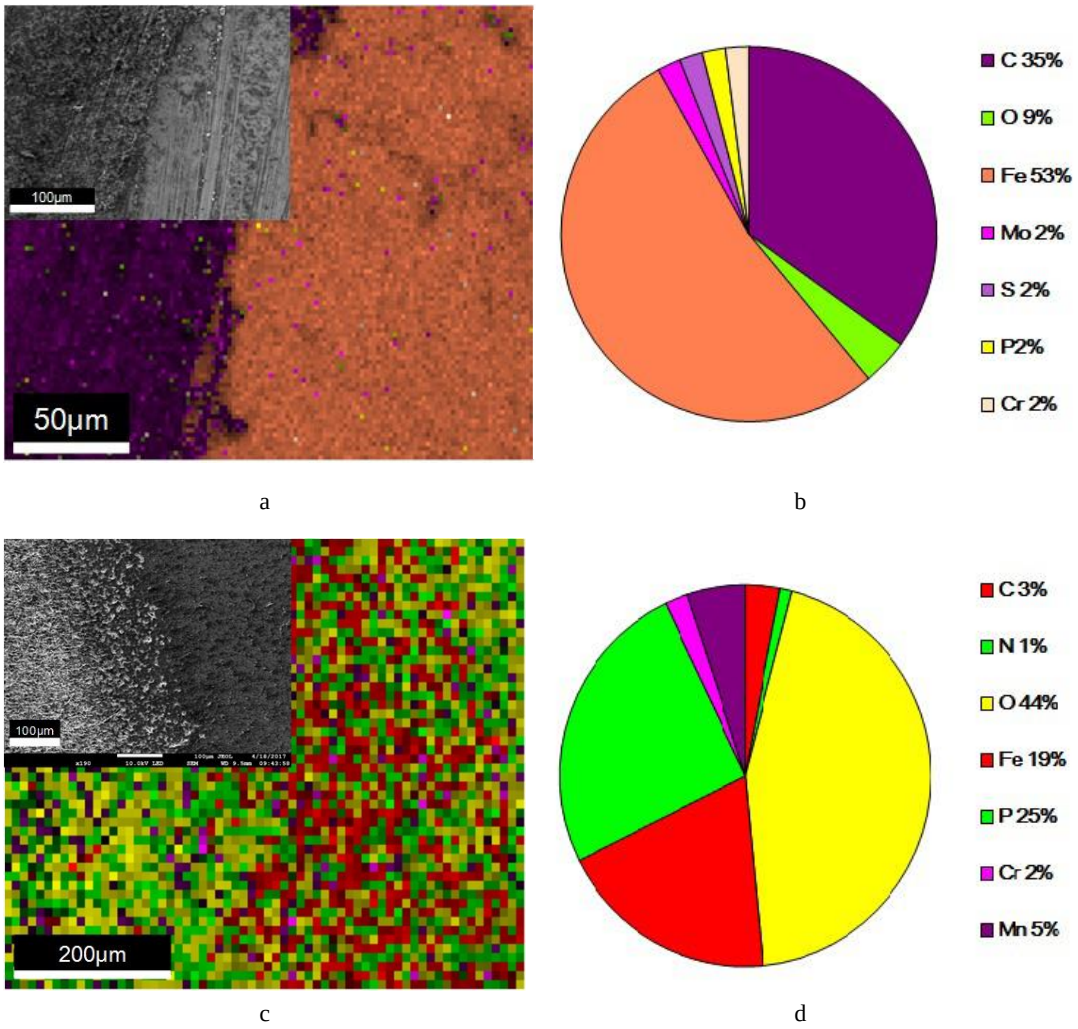

Fig. 12. Analysis of surface energy spectrum components of PC/MoS_2 and Mn–P coating: a – PC/MoS_2 grinding EDS element distribution; b – PC/MoS_2 element content; c – Mn – P coating grinding EDS element distribution; d – Mn – P coating element content

Ref. [20] reported that solid lubricants, such as MoS_2 and graphite, can function as micro balls in the process of friction. According to the surface and interface effect analysis of the material, MoS_2 possesses a large number of dangling keys, exhibiting high chemical instability and reactivity; under the joint action of positive pressure and friction, MoS_2 is easily adsorbed on the friction surface to form a solid lubricating film. Molybdenum disulfide is easily oxidized during the wear process [21], but can prevent the surface adhesion of composite materials and metal materials, thereby effectively improving the wear resistance of the material. The layer structure of graphite reduces the frictional resistance of the friction pair and can effectively reduce friction coefficient and wear amount. Li and Wang reported that MoS_2 exerts a synergistic effect on reducing friction [22, 23]. Furthermore, graphite/MoS_2 composite spraying hard ceramic particles on the substrate enanle to obtain the surface hardening layer. The mechanism of ceramic balls is similar to that of particle shot peening, which results in dense surface to obtain an improved wear resistance [24].

The antifriction mechanism of the manganese phosphate conversion coating is mainly manifested in the fine adsorption of phosphate film micropores in the Fig. 11 b. The capacity to store lubricating oil improves the lubrication characteristics of the friction surface; after running-in, the “bump” rough peaks of the friction surface are quickly smoothed, the surface becomes smooth, and surface roughness is reduced. In the wear phase of the manganese phosphate conversion coating, the distribution of the coating alloy elements on the grinding surface is illustrated by the EDS of the B-points on the worn surfaces (Fig. 12 b and d). The contents of phosphorus and manganese are very high in the pores; the coating is not worn, and the distribution of the “point” of the phosphate film on the worn surface functionsas oil storage and lubrication to prevent direct contact between the metal surface and adhesion wear [25]. The increase in phosphorus content can gradually smooth the friction surface because of the change in the material microstructure structure caused by phosphorus (appearance of martensite) and the effect on the toughness and hardness of iron-based materials; thus, the shearing properties and adhesion resistance of the matrix material during friction action are improved. Similarly, M. Hamiuddin and D. Ernens concluded that phosphorus can significantly

improve the wear-resistance of iron-based materials [26, 27].

4.CONCLUSIONS

1. After surface modification of PC/MoS_2 coating, a solid self-lubricant adheres on the surface of the base material, a solid lubricant adheres on the substrate surface, with a relatively loose coating structure. The solid lubrication medium forms under a high load; in the substrate material interface from the lubricant material, Mo, S, C, and other elements spread to the substrate surface at 20 μm depth, strengthening the matrix. The transformation coating of manganese phosphate is irregularly scaled, the coating is denser, and the grain size starts from 0.5 μm. The surface contains a small number of pores, and the matrix interface is enriched with P, Mn, and other elements, which can improve the formation of the lubricating oil film.
2. In the early run-in stage, PC/MoS_2 and manganese phosphate coating exert an evident antifriction; in the constant grinding phase, the effect of PC/MoS_2 is more prominent. Manganese phosphate conversion coating exhibits a flake porous structure, which can store lubricating oil and is good for oil film formation. The immersion lubrication exhibits better properties of antifriction and wear resistance. By employing solid lubricants MoS_2, C, and other lubrication characteristics, PC/MoS_2 reduces the friction coefficient of contact pairs. In the aspect of extreme pressure characteristics, PC/MoS_2 exhibits a high extreme pressure antiwear property, and the extreme pressure characteristics are slightly improved by 60% compared with the unprocessed surface under the same experimental conditions. The tribological performance and interfacial mechanism of two different surface modifications will provide a basis for further research on the surface modification of gears and bearings.
3. Comparison of the two kinds of surface modification for preparation indicates that the manganese phosphate coating requires simple preparation procedure, short processing period, and low cost, which are suitable for large-scale application. By contrast, PC/MoS_2 spraying features relatively complex equipment and process, high cost, and higher requirements of processing specimens.

Acknowledgments

This work is supported by the National Key R&D Program of China (2017YFB0102400), National Natural Science Foundation of China (NSFC, No. 51705128) and Innovation Project of Graduate Students of Hebei Province (CXZZBS2018036). The authors are especially grateful for the help of Hangzhou Well-test Metal Technology Co., Ltd Mr Boren Xue and Shanghai Parkerizing Co., Ltd. Mr Jianming Chen for sharing their knowledge on graphite/MoS_2 composite coating and phosphate conversion coatings and the preparation of the lab specimens.

REFERENCES

1. **Fernandes, C.M.C.G., Marques, P.M.T., Martins, R.C., Seabra, J.H.O.** Gearbox Power Loss Part II: Friction Losses in Gears *Tribology International* 88 2015: pp. 309 – 316. https://doi.org/10.1016/j.triboint.2014.12.004
2. **Dengo, C., Meneghetti, G., Dabalà, M.** Experimental Analysis of Bending Fatigue Strength of Plain and Notched Case-Hardened Gear Steels *International Journal of Fatigue* 80 (1 – 2) 2015: pp. 145 – 161. https://doi.org/10.1016/j.ijfatigue.2015.04.015
3. **Savaria, V., Monajati, H., Bridier, F., Bocher, P.** Measurement and Correction of Residual Stress Gradients in Aeronautical Gears after Various Induction Surface Hardening Treatments *Journal of Materials Processing Technology* 220 2015: pp. 113 – 123. https://doi.org/10.1016/j.jmatprotec.2014.12.009
4. **Chen, Y., Zang, L.B., Ju, D.Y., Jia, S.** Research Status and Development Trend on Strengthening Technology of High Strength Automobile Gear Surface *China Surface Engineering* 30 (1) 2017: pp. 1 – 15. https://doi: 10.11933/j.issn.1007−9289.20161013003
5. **Gong, T., Yao, P., Zuo, X., Zhang, Z., Xiao, Y., Zhao, L., Zhou, H., Deng, M., Wang, Q., Zhong, A.** Influence of WC Carbide Particle Size on the Microstructure and Abrasive Wear Behavior of WC–10Co–4Cr Coatings for Aircraft Landing Gear *Wear* s362 – 363 2016: pp. 135 – 145. https://doi.org/10.1016/j.wear.2016.05.022
6. **Moorthy, V., Shaw, B.A.** Effect of as-Ground Surface and the BALINIT® C and Nb–S Coatings on Contact Fatigue Damage in gears *Tribology International* 51 (51) 2012: pp. 61 – 70. https://doi.org/10.1016/j.triboint.2012.02.025
7. **Correa, C., Peral, D., Porro, J.A., Diaz, M., Ruiz, L., García-Beltrán, A., Ocañaab, J.l.** Random-type Scanning Patterns in Laser Shock Peening without Absorbing Coating in 2024-T351 Al alloy: A Solution to Reduce Residual Stress Anisotropy *Optics & Laser Technology* 73 2015: pp. 179 – 187. https://doi.org/10.1016/j.optlastec.2015.04.027
8. **Marteau, J., Bigerelle, M., Mazeran, P.E., Bouvier, S.** Relation between Roughness and Processing Conditions of AISI 316L Stainless Steel Treated by Ultrasonic Shot Peening *Tribology International* 82 2014: pp. 319 – 329. https://doi.org/10.1016/j.triboint.2014.07.013
9. **Kameyama, Y., Nishimura, K., Sato, H., Shimpo, R.** Effect of Fine Particle Peening Using Carbon-black/Steel Hybridized Particles on Tribological Properties of Stainless Steel *Tribology International* 78 (4) 2014: pp. 115 – 124. https://doi.org/10.1016/j.triboint.2014.05.006
10. **Kim, S.J., Hyun, K.Y., Jang, S.K.** Effects of Water Cavitation Peening on Electrochemical Characteristic by Using Micro-Droplet Cell of Al–Mg Alloy *Current Applied Physics* 12 (9) 2012: pp: S24 – S30. https://doi.org/10.1016/j.cap.2012.02.013
11. **Lin, S.S., Zhou, K.S., Dai, M.J., Hu, F., Shi, Q., Hou, H.J., Wei, C.B., Li, F.Q., Tong, X.** Effects of Surface Roughness of Substrate on Properties of Ti/TiN/Zr/ZrN Multilayer Coatings *Transactions of Nonferrous Metals Society of China* 25 (2) 2015: pp. 451 – 456. https://doi.org/10.1016/S1003-6326(15)63623-8
12. **Tuszynski, W., Michalczewski, R., Szczerek, M., Kalbarczyk, M.** A New Scuffing Shock Test Method for the Determination of the Resistance to Scuffing of Coated

Gears *Archives of Civil & Mechanical Engineering* 12 (4) 2012: pp. 436 – 445. https://doi.org/10.1016/j.acme.2012.08.003

13. **Lv, Y., Lei, L., Sun, L.** Influence of Different Combined Severe Shot Peening and Laser Surface Melting Treatments on the Fatigue Performance of 20CrMnTi Steel Gear *Materials Science & Engineering A* 658 2016: pp. 77 – 85. https://doi.org/10.1016/j.msea.2016.01.050
14. **Shi, W.K., Jiang, H.W., Qin, D.T., Chen, Y.** Friction and Wear Performance of Superfine Manganous Phosphate Conversion Coating *Tribology* 29 (3) 2009: pp. 267 – 271. https://doi.org/10.16078/j.tribology.2009.03.006
15. **Chen, Y., Yamamoto, A., Omori, K.** Improvement of Contact Fatigue Strength of Gears by Tooth Surface Modification Processing *12th IFToMM World Congress* 2007: p. 6. https://www.victor-aviation.com/pdf/ParkerA184.pdf
16. **De Mello, J.D.B., Costa, H.L., Binder, R.** Friction and Wear Behaviour of Steam-oxidized Sintered Iron Components Coated with Manganese Phosphate *Wear* 263 (1) 2007: pp. 842 – 848. https://doi.org/10.1016/j.wear.2007.01.062
17. **Wang, C.M., Liau, H.C., Tsai, W.T.** Effects of Temperature and Applied Potential on the Microstructure and Electrochemical Behavior of Manganese Phosphate Coating *Surface & Coatings Technology* 201 (6) 2006: pp. 2994 – 3001. https://doi.org/10.1016/j.surfcoat.2006.06.010
18. **Brandão, J.A., Seabra, J.H.O., Castro, M.J.D.** Surface Fitting of an Involute Spur Gear Tooth Flank Roughness Measurement to its Nominal Shape *Measurement* 91 2016: pp. 479 – 487. https://doi.org/10.1016/j.measurement.2016.05.076
19. **Wen, S.Z., Huang, P.** Principles of Tribology (Fourth Edition) Beijing, China *Tsinghua University Press* 2012: pp. 290 – 296.
20. **Santillo, G., Deorsola, F.A., Bensaid, S., Russo, N., Fino, D.** MoS_2 Nanoparticle Precipitation in Turbulent Micromixers *Chemical Engineering Journal* 207 – 208 (5) 2012: pp. 322 – 328. https://doi.org/10.1016/j.cej.2012.06.127
21. **Kovalchenko, A.M., Fushchich, O.I., Danyluk, S.** The Tribological Properties and Mechanism of Wear of Cu-Based Sintered Powder Materials Containing Molybdenum Disulfide and Molybdenum Diselenite under Unlubricated Sliding Against Copper *Wear* s290 – 291 (7) 2012: pp. 106 – 123. https://doi.org/10.1016/j.wear.2012.05.001
22. **Li, X., Gao, Y., Xing, J., Fang, L.** Wear Reduction Mechanism of Graphite and MoS_2 in Epoxy Composites *Wear* 257 (3 – 4) 2004: pp. 279 – 283. https://doi.org/10.1016/j.wear.2003.12.012
23. **Wang, Y.M., Zhou, H.D., Chen, J.M., Ye, Y.P.** Preparation and Friction and Wear Behavior of Waterborne Epoxy Resin-Based Bonded Solid Lubricant Coatings *Tribology* 30 (6) 2010: pp. 577 – 583. http://doi:10.16078/j.tribology.2010.06.011
24. **Zhang, J., Li, W., Wang, H., Song, Q.P., Lu, L.T., Wang, W.J., Liu, Z.W.** A Comparison of the Effects of Traditional Shot Peening and Micro-shot Peening on the Scuffing Resistance of Carburized and Quenched Gear Steel *Wear* s368 – 369 2016: pp. 253 – 257. https://doi.org/10.1016/j.wear.2016.09.029
25. **Lee, Y.L., Chu, Y.R., Li, W.C., Lin, C.S.** Effect of Permanganate Concentration on the Formation and Properties of Phosphate/Permanganate Conversion Coating on AZ31 Magnesium Alloy *Corrosion Science* 70 (70) 2013: pp. 74 – 81. https://doi.org/10.1016/j.corsci.2013.01.014
26. **Jiao, M.H., Su, B.W., Ma, S.B., Wang, B.C., Yin, Y.G. I**nfluence of Phosphorous on the Tribological Properties of PM Iron-Based Sintered Composites *Applied Mechanics & Materials* 217 – 219 2012: pp. 105 – 109. https://doi.org/10.4028/www.scientific.net/AMM.217-219.105
27. **Ernens, D., Rooij, M.B.D., Pasaribu, H.R., Riet, E.J.V., Haaften, W.M.V., Schipper, D.J.** Mechanical Characterization and Single Asperity Scratch Behaviour of Dry Zinc and Manganese Phosphate Coatings *Tribology International* 118 2018: pp. 474 – 483. https://doi.org/10.1016/j.triboint.2017.04.034